

Recent advances in terahertz technology for biomedical applications

Qiushuo Sun¹, Yuezhi He¹, Kai Liu¹, Shuting Fan², Edward P. J. Parrott¹, Emma Pickwell-MacPherson¹

¹Department of Electronic Engineering, The Chinese University of Hong Kong, Shatin, N.T, Hong Kong SAR, China; ²School of Physics and Astrophysics (M013), The University of Western Australia Perth, WA 6009, Australia

Correspondence to: Emma Pickwell-MacPherson, Associate Professor. Rm 426 Ho Sin Hang Engineering Building, Department of Electronic Engineering, The Chinese University of Hong Kong, Shatin, Hong Kong, China. Email: emma@ee.cuhk.edu.hk

Abstract: Terahertz instrumentation has improved significantly in recent years such that THz imaging systems have become more affordable and easier to use. THz systems can now be operated by non-THz experts greatly facilitating research into many potential applications. Due to the non-ionising nature of THz light and its high sensitivity to soft tissues, there is an increasing interest in biomedical applications including both *in vivo* and *ex vivo* studies. Additionally, research continues into understanding the origin of contrast and how to interpret terahertz biomedical images. This short review highlights some of the recent work in these areas and suggests some future research directions.

Keywords: Terahertz imaging; terahertz spectroscopy; cancer imaging; biological contrast; terahertz modelling

Submitted May 08, 2017. Accepted for publication May 25, 2017.

doi: 10.21037/qims.2017.06.02

View this article at: <http://dx.doi.org/10.21037/qims.2017.06.02>

Introduction

Terahertz (THz) light (Tera = 10^{12} , 1 THz = 1×10^{12} Hz) is a million times lower frequency than X rays and is non-ionising. Therefore, it would be safe and desirable to use THz light for medical imaging for both screening and diagnostic purposes if the technology could be developed appropriately. THz light is strongly absorbed by intermolecular bonds e.g., hydrogen bonds present in water and N-H bonds present in proteins. This means it is very sensitive to subtle changes such as increased water content or blood flow which could be due to the presence of disease. THz light is also able to probe the molecular structure of chemicals and resolve thin layers of materials e.g., pharmaceutical tablet coatings and the stratum corneum of the skin (in certain locations). In this review, we update our previous overviews from 2012 (1) and 2014 (2), and summarise recent findings relevant to advancing the usage of THz imaging for medical applications. In Section 2 we summarise advances in THz biomedical understanding, including work on both the origin of contrast and in tissue

modelling. Sections 3 and 4 discuss new findings from *in vivo* and *ex vivo* studies respectively and in Section 5 we highlight some areas of interest for future study.

New advances in THz biomedical understanding

Origin of contrast

Early studies of the origin of contrast between healthy and diseased tissue in the THz region focused on changes in water content (1,3-5). However, water content differences are not only limited to differences between healthy and diseased tissues; it is often seen that fat and muscle tissue have different THz optical properties, a difference that is dominated by their different water contents (6). Additionally, a recent study of bacteria found in infectious diseases observed significant differences in the THz spectrum of these cells, which was attributed to small changes in water content (7). However, the likelihood that water content variation is not the only cause of contrast has been highlighted in numerous studies (8-10). For example,

in 2010 Sy *et al.* showed that water does not exclusively cause the differences observed in the refractive index and absorption coefficient between healthy and cirrhotic liver tissues, but that structural changes in the cells were responsible in part for the changes in the THz optical properties (9).

In addition to structural changes, it is also likely that the molecular changes between diseased and healthy tissues could affect the THz response. A recent study involving methylated DNA, an aberrant DNA type found in early stage cancers, found it has a distinctive molecular resonance at 1.67 THz. By quantifying the THz spectral amplitudes at 1.67 THz, the degree of DNA methylation is ascertained and these results matched the gold-standard commercial enzyme-linked immunosorbent assay (ELISA) like reaction

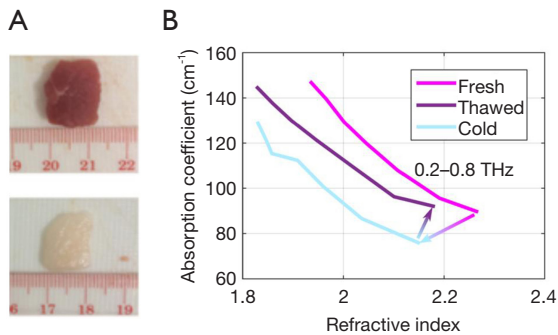


Figure 1 Demonstrating the hysteresis effect due to slow freeze/thaw cycles in porcine tissue. (A) Optical images of the fresh porcine muscle and fat samples; (B) absorption coefficient vs refractive index for fresh, frozen and thawed porcine muscle samples. Adapted with permission from (6).

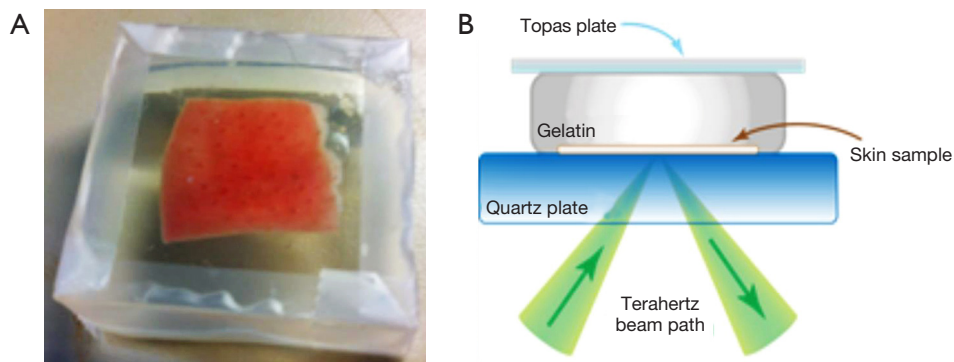


Figure 2 Instead of freezing tissue or removing water content, gelatin embedding presents an alternative way to preserve tissue for terahertz imaging studies. (A) Photograph of gelatin embedded porcine skin; (B) schematic cross-section of the THz measurement of a gelatin embedded sample. Adapted with permission from (12).

method well, and noting greater precision when using THz (11).

Given the observed effects of both water content and structure on the THz optical properties of tissues, the chosen preservation technique and the corresponding effects on both the water content and structure should be carefully considered. Our group has recently reported that slow-freezing a tissue (as opposed to snap-freezing) causes damage to the structure of biological samples which have high water content (such as muscle). This was evident in the hysteresis effect observed in the optical properties of the fresh and thawed porcine samples (shown in *Figure 1A*) when the slow-freezing technique was used (6). The hysteresis in the data is highlighted in *Figure 1B*.

Consequently, a way to preserve the water content of fresh tissue could be useful. In this respect, we investigated the advantages of gelatin embedding freshly excised samples. *Figure 2A* shows a photograph of porcine skin embedded in gelatin. The cross sectional diagram in *Figure 2B* shows how the sample reflectivity is measured in this set up. Gelatin embedding preserved bio samples from dehydration and retained structural integrity for at least 35 hours (12) whereas storing the sample in a petri dish on gauze caused a 10% reduction in the measured absorption coefficient after only 2 hours.

Tissue modelling

Effective media approximations (EMAs) have been widely used to estimate the permittivity of biological tissues. Given the permittivity of the sample and the dehydrated tissue, also called the biological background, the volume fraction

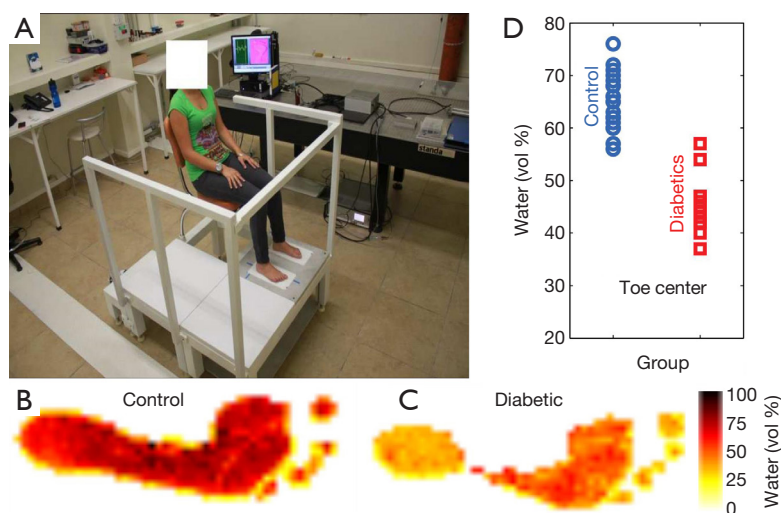


Figure 3 Diabetic foot measurement studies using THz. (A) Photograph of the measurement set-up. THz images plotting the calculated water volume for (B) a control and (C) a diabetic patient. (D) Calculated water volume for control and diabetic patients using data from the centre of the big toe. Adapted with permission from (22).

of water in the sample can be estimated. The Bruggeman model (13) combined with the double Debye model (14,15) and stratified media theory can be used to calculate the reflectivity of samples resembling multi-layer structures (16). This approach has been used successfully *in vivo* on both rat skin (17) and rabbit cornea (18-20). The Bruggeman model is also used to estimate the safety thresholds in the THz range of skin and cornea (21). As well as the Bruggeman model, the Landau-Lifshitz-Looyenga EMA has been used to estimate the THz permittivity of human skin (22). For all EMAs, the accuracy of the underlying material permittivity is crucial. Researchers have used dehydrated tissue to estimate the biological background (16,22), and Debye theory and finite difference time domain (FDTD) methods have been used to model the THz response of breast (23) and skin (24) tissue.

The applicability of THz tissue modelling in a diagnostic context has been recently demonstrated in the screening of diabetic foot syndrome (22). Diabetic foot syndrome causes dehydration of the foot skin, increasing the risk of developing severe ulcers which can eventually necessitate amputation if not treated. A photo of the set up for this *in vivo* study is given in Figure 3A, along with the resulting THz images (Figure 3B, 3C) and classification via water content. Accurate skin modelling allowed the water fraction of the foot skin to be estimated, and a remarkable difference was noted between the diabetic and control groups, particularly in the toe region as plotted in Figure 3D.

Although there is still some overlap between diabetic and control group, researchers are planning a wider and more rigorous clinical trial.

The THz properties of skin are known to vary widely between different locations on the body, resulting from both different hydration levels and structural properties such as stratum corneum thickness (4). In extracting these accurate values for different regions, Zaytsev *et al.* proposed a highly accurate algorithm, considering errors from both imaging window aberrations and digital noise (25). Thus, any technique to measure skin hydration level such as the diabetic foot syndrome study presented earlier (22) needs to be carefully calibrated. This is further complicated by the variability in skin hydration between different patients and, if an imaging plate is used, the occlusion properties of the skin.

The strong attenuation of biological tissue necessitates the use of reflection geometry for THz *in vivo* spectroscopy and imaging. In this context, image registration and measurement repeatability are aided by asking subjects to place the region of interest onto an imaging window (normally made of a low absorption material such as crystalline quartz). However, this window occludes the skin during the measurements, consequently increasing the water concentration in the skin and changing the THz optical properties (26). The decay of the THz signal during the 20 minutes of occlusion was found to be significant, particularly in the first three minutes. Furthermore, the

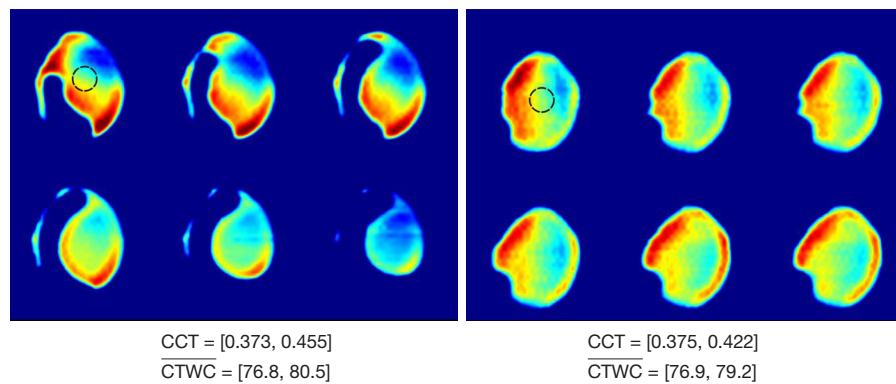


Figure 4 Corneal THz reflectivity maps for two rabbit subjects, with the central corneal thickness (CCT) measurement range in millimetres and corresponding Corneal Tissue Water Content (CTWC) given in percent, supplied from ultrasound measurements. Time increases, from left to right and top to bottom for each image series. The dotted circles overlaid on the top left cornea of each image denote the ultrasound probe location.

occlusion leads to a gradient across the acquired image due to the raster scan induced time differences between the first and last point measured. Sun *et al.* were able to model this amplitude decay using a bi-exponential function (26) and subsequently retrieve the un-occluded image, thereby removing a systematic error from the measurement.

In vivo imaging and spectroscopy

Several studies using *in vivo* THz imaging have essentially been based upon mapping changes in water content. Taylor *et al.* first demonstrated THz imaging of cornea of rabbits *in vivo* using a THz reflection system with central frequency at 0.1 and 0.525 THz respectively. Their experimental results showed that THz imaging could measure the water content in the cornea *in vivo* and that the change on the corneal tissue water content (CTWC) distribution does not necessarily correlate with the corneal central thickness (CCT) (19,20,27). As illustrated in *Figure 4*, the THz reflectivity varies across the cornea, and in the rabbit measurements shown in *Figure 4A* the reflectivity changes the most in regions where the ultrasound probe is not measuring the CCT, suggesting that the CCT will not always be a good measurement of the CTWC. The same group also imaged the fluid shifts caused by burn-induced edemas, comparing the THz results with T2-weighted MRI results (28,29). The THz reflectivity results displayed a high correlation with the MRI results for both partial thickness and full thickness burns; in fact, for partial thickness burns the THz reflectivity demonstrated a greater change and contrast in comparison with the MRI results. The

quantitative method for evaluating the extent of the edema demonstrated in this study suggests that THz spectroscopy could be a powerful diagnostic tool for monitoring burn healing.

Scar healing can also be detected and observed using THz *in vivo* imaging, even when the scars are barely visible by eye. In recent work by the MacPherson group (30), there is clear contrast between the refractive index of the scars and the surrounding skin on four subjects. The healing process of a hypertrophic scar during 6 months post injury is also monitored: whilst contrast in the absorption coefficient decreases with time, the contrast of the refractive index remains significant, as highlighted in *Figure 5*. This work shows the potential of THz to quantitatively measure subtle changes in skin properties noninvasively.

Skin flaps are an important tool for reconstructive surgery: a skin flap is a mass of tissue used for grafting that normally retains its own blood supply during transfer to another site. A recent pilot study using THz spectroscopy shows promise for early assessment (24 hours) of skin flap viability (31). Researchers compare the visible and reflective THz images from 3 bipedicle flaps (flaps which retain a blood supply) and 3 fully excised flaps from rats for seven days post-operation. THz images illustrated the local differences in tissue water content as early as 24 hours post operation whereas visual images required 48 hours before the differences became evident. This is because necrotic excised flaps hold less water in the skin and THz imaging is very sensitive to changes in water content. THz reflection spectroscopy may offer an objective method to evaluate the viability of the tissue flaps instead of the current standard

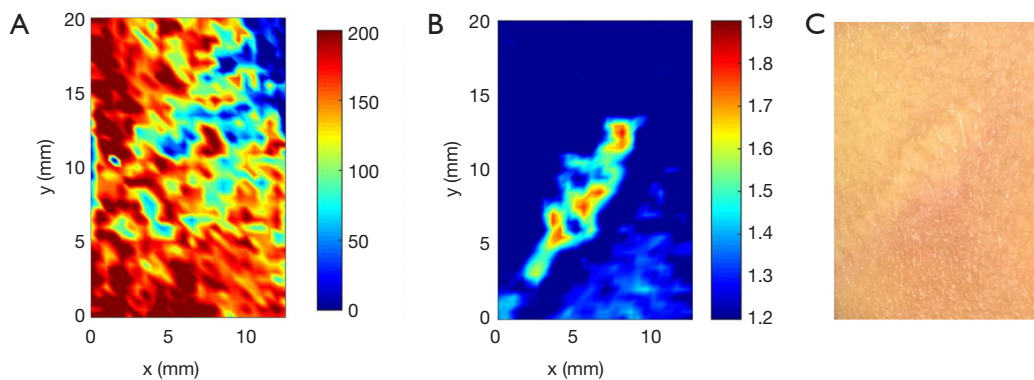


Figure 5 (A) Absorption coefficient, (B) refractive index and (C) visual image of a hypertrophic scar six months post-injury. The refractive index image continues to show significant differences between normal and scarred tissue, which may be indicative of some realignment of collagen fibres in the scarred tissue. Adapted with permission from (30).

which strongly depends on surgeon skill.

Skin melanoma presents itself as a dysplastic nevus (abnormal mole) and survival of this form of cancer depends on early detection. In a recent series of studies Zaytsev *et al.* measured dysplastic and non-dysplastic skin nevi from four patients using *in vivo* THz pulsed spectroscopy and the results show that there are clear differences in the Cole-Cole diagrams of dysplastic and non-dysplastic skin nevi (32-34). These studies demonstrate the importance of investigating different ways to visualize the THz optical properties; in this case the imaginary part of the dielectric permittivity had less obvious differences between dysplastic and non-dysplastic nevi than the real part.

Finally, since *ex vivo* studies of glucose levels in blood (35,36) have shown some promise there has been a move towards developing *in vivo* biosensors for glucose. THz attenuated total reflection (ATR) spectroscopy has shown potential to noninvasively monitor blood glucose levels *in vivo* (37). By monitoring the reflected THz signals from the palms of six healthy subjects a possible correlation between the ATR amplitude and blood glucose concentration was observed. Millimeter wave measurements of rat blood glucose levels *in vivo* have also shown promise in monitoring sugar levels (38) but it remains clear that more work is needed to fully understand the observations. However, *in vivo*, non-invasive monitoring of glucose levels using THz technologies may be possible.

Ex vivo imaging

Ex vivo studies also hold importance particularly for understanding contrast mechanisms and comparing to gold

standards such as histology. Early research by Fitzgerald *et al.* (8) has shown that THz light can differentiate *ex vivo* cancerous breast tissue from the surrounding healthy background. The origin of contrast between diseased and healthy tissue could be different water contents as well as the difference in the cell densities. More recently, in 2015, Bowman *et al.* (39) have investigated the contrast issue by imaging dehydrated breast cancer slides. The samples were formalin fixed, paraffin embedded infiltrating ductal carcinoma (IDC) cut into 10, 20 and 30 μm slides. The reflected amplitude at 1.5 THz was greater for the regions with IDC compared to both the fatty and fibrous parts, see *Figure 6*. Low-power pathology photos like *Figure 6A* reveal that the cell density in IDC regions is generally greater which may be the cause of the greater reflection (red areas) in the THz images (*Figure 6B,6C*). The same group also compared using a transmission setup with reflection geometry in the characterization of breast cancer slides (40). They reported that in a transmission setup, the extraction of THz parameters is less sensitive to phase variation, so the calculation results are more robust whereas in the reflection setup, obtaining an accurate measure of absorption coefficient of fatty tissue is difficult because it is very sensitive to phase error and the flatness of the imaging window. However, reflection mode is more favourable for measuring samples with high absorption, which is true of many tissues, both excised and *in vivo*, due to the high water content.

Similar to the work outlined above, Wahaiia *et al.* (41) report a comparison of transmission images and reflection images, this time focusing on 2 mm thickness paraffin embedded carcinoma-affected colon tissues. The mean

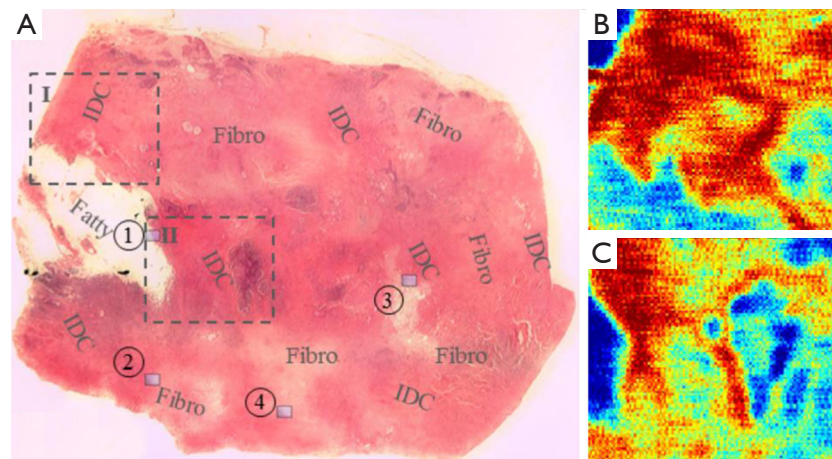


Figure 6 (A) Histology image and high-resolution THz images at 1.5 THz for regions I (B) and II (C). The reflected THz amplitudes for the IDC regions are clearly higher than for the surrounding fatty and fibrous parts.

THz absorption coefficient reported for the colon tumor is 23% greater than the control but is unfortunately still not statistically significant. Since the sample is relatively thick and non-homogenous, the accurate extraction of THz parameters may be challenging, possibly necessitating the further development of THz modalities such as THz ellipsometry.

Oral cancer is easy to be ignored by both doctors and patients because of its typical ulcerous appearance, which leads to many patients missing their optimal treatment timing. The most common diagnostic measure is pathohistological biopsy, but this is a time-consuming examination with a dimensional limitation and must be observed from the perpendicular plane without horizontal bio-information. Thus, a better method which can obtain more diagnostic information should be developed for oral cancer detection, particularly early stage. In 2013 Sim *et al.* (42,43) imaged seven freshly excised oral cancer tissues and an oral malignant melanoma tissue using THz radiation at both 20 and -20°C . THz imaging of both types of frozen tissues had greater sensitivity in the cancerous areas (as identified by histology) compared to adjacent healthy tissue and a larger difference in the refractive index and absorption coefficient between the oral cancer and normal mucosa at -20°C was observed. The greater specificity of the frozen samples was attributed to the removal of water, which links back to the studies of the origin of contrast mentioned in Section 2.1, but a dehydrated control is needed to evaluate this hypothesis.

Research still continues into cancerous tissue and

other tissues of the body in order to build up a better understanding of the factors affecting the THz response. For example, normal gastrointestinal (GI) tract tissues from rats were recently measured using THz reflection imaging and spectroscopy *ex vivo* (25). The distinctively low water concentration in the stratified squamous epithelia (SSE) results in a different reflected THz signal and spectrum when compared to those of other GI tract tissues, again highlighting the importance of water concentration in THz contrast.

Finally, coherent imaging based on THz QCL interferometry has recently emerged, providing an alternative higher frequency technique to the sources of either low frequency and high power, or of low power and broadband nature. A THz QCL source operating at 2.59 THz with the emitted power ranging from ~ 290 to $730\ \mu\text{W}$ has been shown to discriminate different types of porcine tissue: epidermis, upper dermis and lower dermis of skin, muscle and sub-dermal fat, including being able to discern sub-surface features such as blood vessels that are not apparent on the optical images (26).

Future challenges

There have been several advances in understanding the origin of contrast in the past few years, but there is still somewhat of a gap in the available technology to capture fast, accurate terahertz images. Two key areas that should be focused on in the future are imaging speed, and imaging resolution.

Imaging speed

Many THz imaging systems currently use raster scanning to capture the region of interest. In this technique, a single source and receiver are scanned over a sample, measuring the terahertz signal at each point sequentially. Consequently, images take many seconds to acquire, ranging between a few seconds to a few minutes depending on the required signal to noise ratio and image resolution. This length of time for acquisition severely limits *in vivo* measurements in particular, as the sample needs to be kept mechanically stable for a long time. Furthermore, if occlusion is an issue as shown earlier (16), the region of interest may give erroneous data due to the dynamic nature of the sample and the sequential process of acquisition. One option to increase imaging speed is to synchronously acquire multiple pixels at once through the use of an array of emitters and/or detectors and there have been some significant improvements presented recently on the development of efficient microbolometer arrays for detection (44-46). However, such arrays are not suitable for time-domain imaging as they have limited ability to capture the spectral information available, and arrays of time-domain sources and detectors remain expensive and difficult to fabricate.

Another option therefore is to alter the imaging paradigm itself, relying on the sparsity of spatial frequencies in most images to perform compressed sensing (CS). First demonstrated at THz frequencies in 2008 (47,48) this technique has since been demonstrated, among others, by using either random mechanically developed and switched masks (49), a spinning disk set (50), electrically gated graphene modulator arrays (51) and by photoexciting a silicon substrate with an optical pattern (52). The techniques demonstrated here rely on a binary state for each pixel, i.e., the pixels are either on and off, in order to eventually separate the response of each pixel through the linear combinations recorded in the measurements. If a true on and off state cannot be achieved, then this results in a reduced signal-to-noise ratio. With the exception of the mechanically derived patterns (such as different cards that can be swapped in and out by hand, or the prefabricated spinning discs) current demonstrations have suffered from a relatively low modulation depth [around 50% at the most (51)]. Recently however, our group has developed and demonstrated a new modulation paradigm that is based around modulating a conductive interface at a total internally reflected (TIR) surface (53,54) (Figure 7). This technique allows one to modulate a THz pixel close to

100% using either electrical or optical control (depending on the nature of the conductive interface), which will greatly enhance the possible use of CS in THz point source imaging. Techniques such as this may allow imaging speeds approaching single second acquisition times to be possible in the near future.

Imaging resolution

In the far field, the imaging resolution of a THz measurement is generally limited to the wavelength of the light, which is of the order of hundreds of microns in the THz range. Therefore, THz imaging of biological structures such as individual cells are not possible using far-field techniques that have been the focus of the previously mentioned articles. Near-field imaging however, whereby the evanescent wave is probed, makes it possible to beat the diffraction limit and achieve sub-wavelength resolution imaging (55). This has been used to study carrier concentration in semiconductors, fundamental physics of metamaterials, and radially polarized beam profiles (56-59). Using such techniques in a biomedical context will improve our understanding of cellular composition and may help further understand the origin of context. Recent near-field imaging studies of leaves and insects at 1.0422 THz have achieved a pixel size of 35x35 μm , almost 10 times smaller than the wavelength of the THz light (60). This is already approaching the size of human cells, and as near-field techniques move towards the nanoscale (56) in biomedical contexts it may become possible to probe the structure of cells themselves with THz light.

Conclusions

Since our 2012 review (1) there has continued to be significant progress in developing THz technology for use in biomedical fields of study. This has been driven in part by the increased availability and affordability of turn-key THz systems to research groups around the world. For both *in vivo* and *ex vivo* imaging and spectroscopy, progress has been made in understanding the origins of contrast and in methods to improve contrast between healthy and diseased tissues. In particular, *ex vivo* techniques have focused on studying the effects of removing water from tissues to understand further the role of hydration in the observed differences between healthy and diseased tissues. These excised tissue studies can be compared with gold-standard histology which is a key step in demonstrating the viability

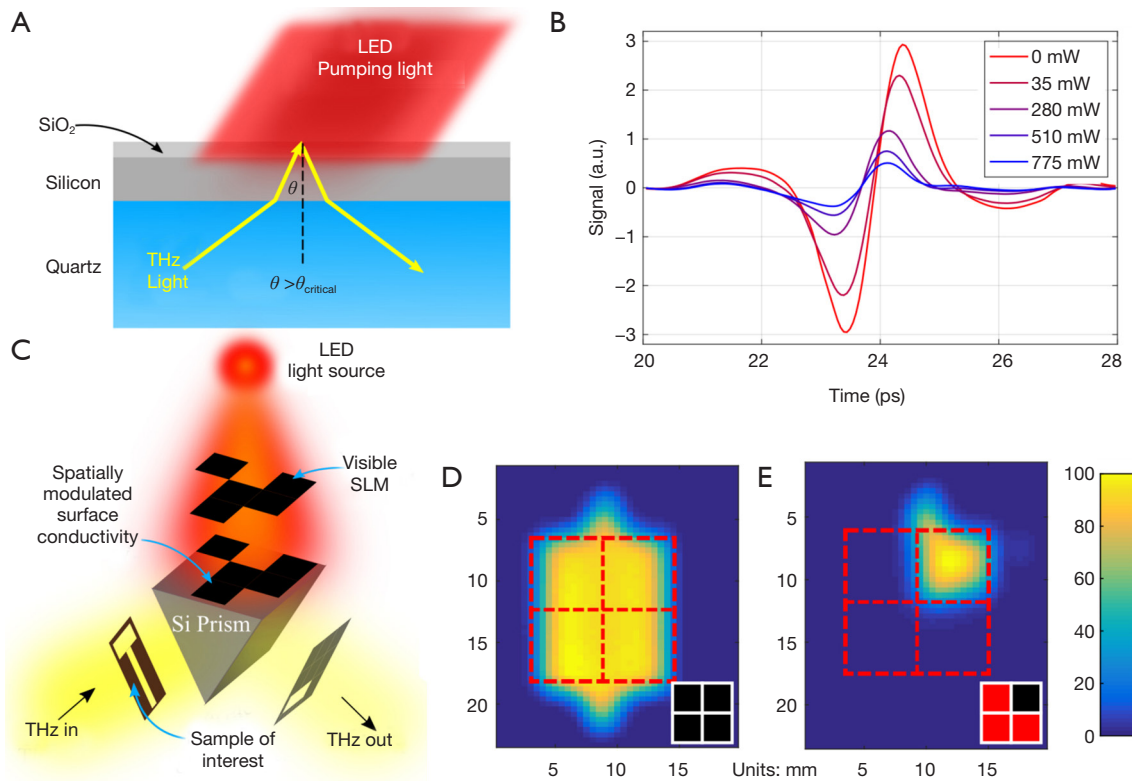


Figure 7 (A) Schematic of the TIR optical pumping THz modulator (B) TIR signal for different optical pumping powers. In (C) a schematic of a proposed compressed sensing imaging system based upon this approach is shown. (D,E) show the reflected THz intensity when either no optical light is incident upon the TIR interface, or when optical light is pumping three of the four quadrants as shown by the dotted lines and the inset legends (black: light off, red: light on), thereby demonstrating the potential for spatial modulation. Adapted from (53).

of THz technology. Because of its importance in affecting the THz properties of tissues, removing the water does generally reduce the differentiation between healthy and diseased tissue, yet it is possible that dehydrated samples suffer less from the natural variations in hydration present between different subjects. In probing such samples, it may be possible to glean some structural understanding of diseased and healthy tissue, leading in the long run to both clinical discoveries and more robust *in vivo* measurements.

From the *in vivo* standpoint, the key bottleneck still appears to be imaging speed and image registration. As has been seen with our occlusion studies, a long measurement time for an area leads to a systematic shift in the measured THz response, and given the previously reported dependency on water content this has the potential to render accurate detection of healthy and diseased tissues challenging. Furthermore, the slower the measurement the longer the subject must remain still and in good contact with the imaging window, which has knock on effects to the

quality of the image registration as well as exacerbating the issues of pressure which have not as of yet been carefully studied in this frequency range. Improvements in THz imaging speed, and the quest to develop a near-video rate imaging system for THz spectroscopy will help to dispel some of these issues, and it is expected that research groups worldwide will continue to push the limits of imaging speed. Finally, the wavelength of THz light does impact the resolution of the images and by extension limits the minimum size of THz pixels to the high sub-millimeter range at best (in the far field). It is possible that future near-field imaging may allow us to both differentiate tissue margins and also, and perhaps more importantly, further understand the underlying origins of contrast beyond the hydration state.

Acknowledgements

Funding: This work was supported by the Hong Kong

Innovation and Technology Scheme (ITS/371/16), the Research Grants Council of Hong Kong (projects 14205514 and 14201415) and the Hong Kong PhD Fellowship Scheme.

Footnote

Conflicts of Interest: The authors have no conflicts of interest to declare.

References

1. Yu C, Fan S, Sun Y, Pickwell-MacPherson E. The potential of terahertz imaging for cancer diagnosis: A review of investigations to date. *Quant Imaging Med Surg* 2012;2:33-45.
2. Fan S, He Y, Ung BS, Pickwell-MacPherson E. The growth of biomedical terahertz research. *J Phys D Appl Phys* 2014;47:374009.
3. Ashworth PC, Pickwell-MacPherson E, Provenzano E, Pinder SE, Purushotham AD, Pepper M, Wallace VP. Terahertz pulsed spectroscopy of freshly excised human breast cancer. *Opt Express* 2009;17:12444-54.
4. Pickwell E, Cole BE, Fitzgerald AJ, Pepper M, Wallace VP. In vivo study of human skin using pulsed terahertz radiation.
5. Son JH. Terahertz electromagnetic interactions with biological matter and their applications. *J Appl Phys* 2009;105:102033.
6. He Y, Ung BS, Parrott EP, Ahuja AT, Pickwell-MacPherson E. Freeze-thaw hysteresis effects in terahertz imaging of biomedical tissues. *Biomed Opt Express* 2016;7:4711.
7. Yang X, Wei D, Yan S, Liu Y, Yu S, Zhang M, Yang Z, Zhu X, Huang Q, Cui HL, Fu W. Rapid and label-free detection and assessment of bacteria by terahertz time-domain spectroscopy. *J Biophotonics* 2016;9:1050-8.
8. Fitzgerald AJ, Wallace VP, Jimenez-Linan M, Bobrow L, Pye RJ, Purushotham AD, Arnone DD. Terahertz pulsed imaging of human breast tumors. *Radiology* 2006;239:533-40.
9. Sy S, Huang S, Wang YX, Yu J, Ahuja AT, Zhang YT, Pickwell-Macpherson E. Terahertz spectroscopy of liver cirrhosis: investigating the origin of contrast. *Phys Med Biol* 2010;55:7587-96.
10. Wahaia F, Valusis G, Bernardo LM, Almeida A, Moreira JA, Lopes PC, MacUtkovic J, Kasalynas I, Seliuta D, Adomavicius R, Henrique R, Lopes MH. Detection of colon cancer by terahertz techniques. *J Mol Struct* 2011;1006:77-82.
11. Cheon H, Yang H, Lee SH, Kim YA, Son JH. Terahertz molecular resonance of cancer DNA. *Sci Rep* 2016;6:37103.
12. Fan S, Ung B, Parrott EP, Pickwell-MacPherson E. Gelatin embedding: a novel way to preserve biological samples for terahertz imaging and spectroscopy. *Phys Med Biol* 2015;60:2703-13.
13. Bruggeman DA. Berechnung verschiedener physikalischer Konstanten von heterogenen Substanzen. I. Dielektrizitätskonstanten und Leitfähigkeiten der Mischkörper aus isotropen Substanzen. *Ann Phys* 1935;416:636-64.
14. Debye P. Einige Resultate einer kinetischen Theorie der Isolatoren. *Phys Zeitschrift* 1912;13:97-100.
15. Pickwell E, Cole BE, Fitzgerald AJ, Wallace VP, Pepper M. Simulation of terahertz pulse propagation in biological systems. *Appl Phys Lett* 2004;84:2190.
16. Bennett DB, Li W, Taylor ZD, Grundfest WS, Brown ER. Stratified Media Model for Terahertz Reflectometry of the Skin. *IEEE Sens J* 2011;11:1253-62.
17. Tewari P, Kealey CP, Bennett DB, Bajwa N, Barnett KS, Singh RS, Culjat MO, Stojadinovic A, Grundfest WS, Taylor ZD. In vivo terahertz imaging of rat skin burns. *J Biomed Opt* 2012;17:040503.
18. Bennett D, Taylor Z, Tewari P, Sung S, Maccabi A, Singh R, Culjat M, Grundfest W, Hubschman JP, Brown E. Assessment of corneal hydration sensing in the terahertz band: in vivo results at 100 GHz. *J Biomed Opt* 2012;17:97008-1.
19. Taylor ZD, Garritano J, Sung S, Bajwa N, Bennett DB, Nowroozi B, Tewari P, Sayre JW, Hubschman JP, Deng SX, Brown ER, Grundfest WS. THz and mm-wave sensing of corneal tissue water content: In vivo sensing and imaging results. *IEEE Trans Terahertz Sci Technol* 2015;5:184-96.
20. Taylor ZD, Garritano J, Sung S, Bajwa N, Bennett DB, Nowroozi B, Tewari P, Sayre J, Hubschman JP, Deng S, Brown ER, Grundfest WS. THz and mm-wave sensing of corneal tissue water content: Electromagnetic modeling and analysis. *IEEE Trans Terahertz Sci Technol* 2015;5:170-83.
21. Saviz M, Spathmann O, Streckert J, Hansen V, Clemens M, Faraji-Dana R. Theoretical estimations of safety thresholds for terahertz exposure of surface tissues. *IEEE Trans Terahertz Sci Technol* 2013;3:635-40.
22. Hernandez-Cardoso GG, Rojas-Landeros SC, Alfaro-

- Gomez M, Hernandez-Serrano AI, Salas-Gutierrez I, Lemus-Bedolla E, Castillo-Guzman AR, Lopez-Lemus HL, Castro-Camus E. Terahertz imaging for early screening of diabetic foot syndrome: A proof of concept. *Sci Rep* 2017;7:42124.
23. Fitzgerald AJ, Pickwell-MacPherson E, Wallace VP. Use of Finite Difference Time Domain Simulations and Debye Theory for Modelling the Terahertz Reflection Response of Normal and Tumour Breast Tissue. *PLoS One* 2014;9:e99291.
 24. Truong BC, Tuan HD, Kha HH, Nguyen HT. Debye parameter extraction for characterizing interaction of terahertz radiation with human skin tissue. *IEEE Trans Biomed Eng* 2013;60:1528-37.
 25. Zaytsev KI, Gavidush AA, Chernomyrdin NV, Yurchenko SO. Highly Accurate in Vivo Terahertz Spectroscopy of Healthy Skin: Variation of Refractive Index and Absorption Coefficient Along the Human Body. *IEEE Trans Terahertz Sci Technol* 2015;5:817-27.
 26. Sun Q, He Y, Parrott EP, Pickwell-MacPherson E. In vivo THz imaging of human skin: Accounting for occlusion effects. In: 2016 41st International Conference on Infrared, Millimeter, and Terahertz waves (IRMMW-THz). IEEE 2016:1-2.
 27. Sung S, Chantra S, Bajwa N, McCurdy R, Kerezyte G, Garritano J, Hubschman JP, Grundfest W, Deng SX, Taylor ZD. Direct measurement of corneal tissue water content by reflection imaging at Terahertz Frequencies. *Invest Ophthalmol Vis Sci* 2015;56:1644.
 28. Bajwa N, Sung S, Ennis DB, Fishbein MC, Nowroozi B, Ruan D, Maccabi A, Alger J, St John MA, Grundfest WS, Taylor ZD. Terahertz Imaging of Cutaneous Edema: Correlation with Magnetic Resonance Imaging in Burn Wounds. *IEEE Trans Biomed Eng* 2017. Available online: <http://ieeexplore.ieee.org/document/7835228/>
 29. Bajwa N, Sung S, Garritano J, Nowroozi B, Tewari P, Ennis DB, Alger J, Grundfest W, Taylor Z. In vivo confirmation of hydration based contrast mechanisms for terahertz medical imaging using MRI. In: Razeghi M, Baranov AN, Zavada JM, Pavlidis D. editors. *Proc. SPIE 9199, Terahertz Emitters, Receivers, and Applications V*. 2014:91990U.
 30. Fan S, Ung BS, Parrott EP, Wallace VP, Pickwell-MacPherson E. In vivo terahertz reflection imaging of human scars during and after the healing process. *J Biophotonics* 2016. Available online: <http://doi.wiley.com/10.1002/jbio.201600171>
 31. Bajwa N, Au J, Jarraya R, Sung S, Fishbein MC, Riopelle D, Ennis DB, Aghaloo T, St John MA, Grundfest WS, Taylor ZD. Non-invasive terahertz imaging of tissue water content for flap viability assessment. *Biomed Opt Express* 2016;8:460-74.
 32. Zaytsev KI, Kudrin KG, Reshetov IV, Gavidush AA, Chernomyrdin NV, Karasik VE, Yurchenko SO. In vivo spectroscopy of healthy skin and pathology in terahertz frequency range. *J Phys Conf Ser* 2015;584:12023.
 33. Zaytsev KI, Chernomyrdin NV, Kudrin KG, Gavidush AA, Nosov PA, Yurchenko SO, Reshetov IV. In vivo terahertz pulsed spectroscopy of dysplastic and non-dysplastic skin nevi. *J Phys Conf Ser* 2016;735:12076.
 34. Zaytsev KI, Kudrin KG, Karasik VE, Kim Y, Chang MC, Pikov V. In vivo terahertz spectroscopy of pigmented skin nevi: Pilot study of non-invasive early diagnosis of dysplasia. *Appl Phys Lett* 2015;106:53702.
 35. Siegel PH, Tang A, Virbila G, Kim Y, Chang MC, Pikov V. Compact non-invasive millimeter-wave glucose sensor. In: 2015 40th International Conference on Infrared, Millimeter, and Terahertz waves (IRMMW-THz). IEEE 2015:1-3.
 36. Gusev SI, Borovkova MA, Strepitov MA, Khodzitsky MK. Blood optical properties at various glucose level values in THz frequency range. In: Brown JQ, Deckert V. editors. *Proc. SPIE 9537 Clinical and Biomedical Spectroscopy and Imaging IV*. 2015:95372A.
 37. Cherkasova O, Nazarov M, Shkurinov A. Noninvasive blood glucose monitoring in the terahertz frequency range. *Opt Quantum Electron* 2016;48:217.
 38. Siegel PH, Dai W, Kloner RA, Csete M, Pikov V. First millimeter-wave animal in vivo measurements of L-Glucose and D-Glucose: Further steps towards a non-invasive glucometer. In: 2016 41st International Conference on Infrared, Millimeter, and Terahertz waves (IRMMW-THz). IEEE, 2016:1-3.
 39. Bowman TC, El-Shenawee M, Campbell LK. Terahertz Imaging of Excised Breast Tumor Tissue on Paraffin Sections. *IEEE Trans Antennas Propag* 2015;63:2088-97.
 40. Bowman T, El-Shenawee M, Campbell LK. Terahertz transmission vs reflection imaging and model-based characterization for excised breast carcinomas. *Biomed Opt Express* 2016;7:3756-783.
 41. Wahaia F, Kasalynas I, Venckevicius R, Seliuta D, Valusis G, Urbanowicz A, Molis G, Carneiro F, Carvalho Silva CD, Granja PL. Terahertz absorption and reflection imaging of carcinoma-affected colon tissues embedded in paraffin. *J Mol Struct* 2016;1107:214-9.
 42. Sim YC, Park JY, Ahn KM, Park C, Son JH. Terahertz

- imaging of excised oral cancer at frozen temperature. *Biomed Opt Express* 2013;4:1413-21.
43. Sim YC, Ahn KM, Park JY, Park CS, Son JH. Temperature-dependent terahertz imaging of excised oral malignant melanoma. *IEEE J Biomed Health Inform* 2013;17:779-84.
 44. Simoens F, Meilhan J, Nicolas JA. Terahertz Real-Time Imaging Uncooled Arrays Based on Antenna-Coupled Bolometers or FET Developed at CEA-Leti. *J Infrared, Millimeter, Terahertz Waves* 2015;36:961-85.
 45. Lee AW, Wil BS, Kumar S, Qing Hu, Reno JL. Real-time imaging using a 4.3-THz quantum cascade laser and a 320x240 microbolometer focal-plane array. *IEEE Photonics Technol Lett* 2006;18:1415-7.
 46. Oda N. Uncooled bolometer-type Terahertz focal plane array and camera for real-time imaging. *Comptes Rendus Phys* 2010;11:496-509.
 47. Chan WL, Moravec ML, Baraniuk RG, Mittleman DM. Terahertz imaging with compressed sensing and phase retrieval. *Opt Lett* 2008;33:974-6.
 48. Chan WL, Charan K, Takhar D, Kelly KF, Baraniuk RG, Mittleman DM. A single-pixel terahertz imaging system based on compressed sensing. *Appl Phys Lett* 2008;93:121105.
 49. Shen YC, Gan L, Stringer M, Burnett A, Tych K, Shen H, Cunningham JE, Parrott EP, Zeitler JA, Gladden LF, Linfield EH, Davies AG. Terahertz pulsed spectroscopic imaging using optimized binary masks. *Appl Phys Lett* 2009;95:231112.
 50. Shen H, Gan L, Newman N, Dong Y, Li C, Huang Y, Shen YC. Spinning disk for compressive imaging. *Opt Lett* 2012;37:46-8.
 51. Sensale-Rodriguez B, Rafique S, Yan R, Zhu M, Protasenko V, Jena D, Liu L, Xing HG. Terahertz imaging employing graphene modulator arrays. *Opt Express* 2013;21:2324-30.
 52. Busch S, Scherger B, Scheller M, Koch M. Optically controlled terahertz beam steering and imaging. *Opt Lett* 2012;37:1391.
 53. Liu X, Parrott EP, Ung BS, Pickwell-MacPherson E. Exploiting total internal reflection geometry for efficient optical modulation of terahertz light. *APL Photonics* 2016;1:76103.
 54. Liu X, Chen Z, Parrott EP, Ung BS, Xu J, Pickwell-MacPherson E. Graphene Based Terahertz Light Modulator in Total Internal Reflection Geometry. *Adv Opt Mater* 2017;5:1600697.
 55. Cocker T, Jelic V, Gupta M, Molesky SJ, Burgess JA, De Los Reyes G, Titova LV, Tsui YY, Freeman MR, Hegmann FA. An ultrafast terahertz scanning tunnelling microscope. *Nat Photonics* 2013;7:620-5.
 56. Huber AJ, Keilmann F, Wittborn J, Aizpurua J, Hillenbrand R. Terahertz near-field nanoscopy of mobile carriers in single semiconductor nanodevices. *Nano Lett* 2008;8:3766-70.
 57. Cao W, Singh R, Zhang C, Han J, Tonouchi M, Zhang W. Plasmon-induced transparency in metamaterials: Active near field coupling between bright superconducting and dark metallic mode resonators. *Appl Phys Lett* 2013;103:101106.
 58. Tuniz A, Kaltenecker KJ, Fischer BM, Walther M, Fleming SC, Argyros A, Kuhlmeier BT. Metamaterial fibres for subdiffraction imaging and focusing at terahertz frequencies over optically long distances. *Nat Commun* 2013;4:2706.
 59. Kaltenecker KJ, König-Otto JC, Mittendorff M, Winnerl S, Schneider H, Helm M, Helm H, Walther M, Fischer BM. Gouy phase shift of a tightly focused, radially polarized beam. *Optica* 2016;3:35.
 60. Fawole OC, Tabib-Azar M. Terahertz Near-Field Imaging of Biological Samples With Horn Antenna-Excited Probes. *IEEE Sens J* 2016;16:8752-60.

Cite this article as: Sun Q, He Y, Liu K, Fan S, Parrott EP, Pickwell-MacPherson E. Recent advances in terahertz technology for biomedical applications. *Quant Imaging Med Surg* 2017;7(3):345-355. doi: 10.21037/qims.2017.06.02